Radiative corrections to the decay $H^+ \to W^+ A^0$

A.G. Akeroyd[1,a], A. Arhrib[2,3,b], E. Naimi[2,3,c]

[1] KEK Theory Group, Tsukuba, Ibaraki 305-0801, Japan
[2] Département de Mathématiques, Faculté des Sciences et Techniques, B.P 416, Tanger, Morocco
[3] UFR – High Energy Physics, Physics Departement, Faculty of Sciences, P.O. Box 1014, Rabat, Morocco

Abstract. Full one-loop electroweak corrections to the on-shell decay $H^+ \to W^+ A^0$ are computed in the framework of models with two Higgs doublets (THDM). Such a decay may be dominant for $H^{\pm}$ over a wide range of parameter space relevant at present and future colliders. We show that the corrections may approach 40% and in particular are sensitive to λ_5, which parameterizes the discrete symmetry breaking term. We suggest that a measurement of the branching ratio of $H^+ \to W^+ A^0$ may offer a possibility of measuring the magnitude of λ_5.

1. Introduction

The phenomenology of charged Higgs bosons ($H^{\pm}$) has received much attention in recent years [1] since their discovery would provide conclusive evidence of physics beyond the standard model (SM) [2]. Charged Higgs bosons are predicted in many theoretically well-motivated extensions of the SM. The simplest model which contains a $H^{\pm}$ is the two Higgs doublet model (THDM), which is formed by adding an extra complex $SU(2)_{\mathrm{L}} \otimes U(1)_Y$ scalar doublet to the SM lagrangian. Motivations for such a structure include CP-violation in the Higgs sector and a possible solution to the cosmological domain wall problem [3]. In particular, the Higgs sector of the minimal supersymmetric standard model (MSSM) [1] takes the form of a constrained THDM.

The phenomenology of $H^{\pm}$ has received substantial attention at e^+e^- colliders [4,5], hadron colliders [6–8], $\mu^+\mu^-$ colliders [9] and $\gamma\gamma$ colliders [10]. Most phenomenological studies have been carried out in the context of the MSSM. The combined null-searches from all four CERN LEP collaborations derive the lower limit $m_{H^{\pm}} \geq 77.4$ GeV (95% c.l.) [11], a limit which applies to all models in which BR($H^{\pm} \to \tau\nu_{\tau}$)+ BR($H^{\pm} \to cs$) = 1, where BR signifies the branching ratio. Current mass bounds from LEP-II for the neutral pseudoscalar A^0 of the MSSM ($m_A \geq 90.5\,\mathrm{GeV}$) force $m_{H^{\pm}} \geq 120\,\mathrm{GeV}$ in this model [12], which is stronger than the direct search limit above. Limits on $m_{H^{\pm}}$ from the Fermilab Tevatron searches [13] are $\tan\beta$ dependent since a significant BR($t \to H^+b$) is required in order to obtain a visible signal. The limits

are competitive with those from LEP-II for the regions $\tan\beta \leq 1$ or ≥ 40.

In the MSSM, $m_{H^{\pm}}$ and the mass of the pseudoscalar m_A are approximately degenerate for values greater than $200\,\mathrm{GeV}$, and so the two-body decay $H^{\pm} \to A^0 W$ is never allowed for masses of interest at the CERN Large Hadron Collider (LHC). The three-body decay $H^{\pm} \to A^0 W^* \to A^0 f\bar{f}$ is open for smaller $m_{H^{\pm}}$ although it possesses a small branching ratio (BR $\leq 5\%$ for $m_{H^{\pm}} \geq 110\,\mathrm{GeV}$) [14]. Therefore, for masses of interest at the LHC the principal decay channel is $H^{\pm} \to tb$, with decays to SUSY particles possibly open as $m_{H^{\pm}}$ increases [15]. Recently there has been a surge of interest in studies of the MSSM with unconstrained CP-violating phases. In such scenarios H^0–A^0 mixing may be induced radiatively [16] although this only leads to maximum mass splittings of the order $20\,\mathrm{GeV}$ for small values of $\tan\beta$; thus the two-body decay would not be open even in this case.

Non-supersymmetric THDMs (hereafter to be called simply "THDM") have also received considerable attention in the literature. In such models all the Higgs masses may be taken as free parameters (in contrast to the MSSM), thus allowing the possibility of the two-body decay $H^{\pm} \to A^0 W$ for certain choices of m_A and $m_{H^{\pm}}$. This decay mode possesses no mixing angle suppression, in contrast to $H^{\pm} \to h^0 W$, and may compete with conventional decays [17,18]. In fact, in a sizeable region of parameter space we show that it may be the dominant channel. Motivated by the results in [17] the authors calculated in [19] the Yukawa corrections to the decay $H^{\pm} \to A^0 W^{(*)}$ and found that in the on-shell case the corrections may approach 50% for small values of $\tan\beta$. In this paper we complete that analysis and include the full bosonic corrections for the case of the W being on-shell.

[a] e-mail: akeroyd@post.kek.jp
[b] e-mail: arhrib@fstt.ac.ma
[c] e-mail: naimi@fstt.ac.ma

Conventional Higgs searches at LEP-II assume the decays $H^\pm \to \tau \nu_\tau$ and cs [11], although the OPAL collaboration has recently carried out the first search for $H^\pm \to A^0 W^*$ topologies [20] in the context of the THDM (Model I). A recent study [21] showed that the decay $H^\pm \to A^0 W$ offers good chances of detection for $H^\pm$ at the LHC, where an analysis in the context of the MSSM with an extra singlet superfield was carried out (NMSSM). Much of this work would be relevant for the THDM that we consider, although our bosonic corrections would not be directly applicable to the NMSSM, since the latter possesses two more neutral Higgs bosons in addition to different Higgs self-couplings.

This paper is organized as follows. In Sect. 2 we introduce our notation and outline the form of the one-loop corrections. In Sect. 3 we explain the importance of including diagrams with the emission of a soft photon, $H^+ \to W^+ A^0 \gamma$, in order to keep the radiative corrections infra-red finite. Section 4 covers the various experimental and theoretical constraints that we impose. Section 5 presents our numerical results for the full corrections (bosonic and Yukawa), while Sect. 6 contains our conclusions. The explicit form of the corrections is contained in the appendix.

2. Lowest order result and structure of one-loop radiative corrections

2.1. Lowest order result

We will be using the notation and conventions of our previous work [19], which we briefly review here. The momentum of the charged Higgs boson H^+ is denoted by p_H (p_H is incoming), p_W is the momentum of the W^+ gauge boson and p_A the momentum of the CP-odd A^0 (p_W and p_A are outgoing).

The relevant part of the lagrangian describing the interaction of the $W^\pm$ with $H^\pm$ and A^0 comes from the covariant derivative which is given by

$$\mathcal{L} = \frac{e}{2s_{\mathrm{W}}} W^+_\mu (H^- \overset{\leftrightarrow}{\partial}{}^\mu A^0) + \text{h.c.} \qquad (2.1)$$

This interaction is model independent (SUSY or non-SUSY) and depends only on standard parameters: the electric charge (e) and the Weinberg angle ($s_{\mathrm{W}} = \sin \theta_{\mathrm{W}}$).

The lowest-order Feynman diagram for the two-body decay $H^+ \to A^0 W^+$ is depicted in Fig. 1.

In the Born approximation, the decay amplitude of the charged Higgs into an *on-shell CP*-odd Higgs boson A^0 and the gauge boson W^+ (Fig. 1) can be written as

$$\mathcal{M}^0(H^+ \to W^+ A^0) = \epsilon^*_\mu \Gamma^\mu_0, \qquad (2.2)$$

where

$$\Gamma^\mu_0 = \mathrm{i} \frac{e}{2s_{\mathrm{W}}} (p_H + p_A)_\mu.$$

Here ϵ_μ is the $W^\pm$ polarization vector. We then have the following decay width:

$$\Gamma^0_{on} = \frac{\alpha}{16 s^2_{\mathrm{W}} m^2_W m^3_{H^\pm}} \lambda^{\frac{3}{2}}(m^2_{H^\pm}, m^2_A, m^2_W), \quad (2.3)$$
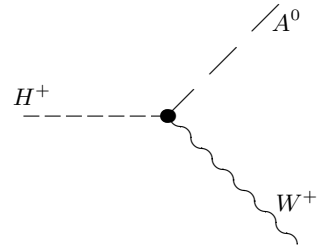

Fig. 1. Lowest-order Feynman diagram for the decay $H^+ \to A^0 W^+$

where $\lambda = \lambda(x, y, z) = x^2 + y^2 + z^2 - 2(xy + xz + yz)$ is the familiar two-body phase space function. Note that in the MSSM the two-body decay of the charged Higgs boson into $W^+ A^0$ is kinematically not allowed. In this paper we will not present results for the case of $W^\pm$ being off-shell. The authors of [19] evaluated the Yukawa corrections in the off-shell case for $m_{H^\pm}$ in the range of LEP-II, finding maximum values of a few percent.

2.2. One-loop radiative corrections

We shall evaluate the bosonic one-loop radiative corrections to the decay $H^+ \to W^+ A^0$, and add them to the Yukawa corrections previously evaluated in [19]. This set of corrections is ultra-violet (UV) and infra-red (IR) divergent. The UV singularities are treated by dimensional regularization [22] in the on-mass-shell renormalization scheme. The IR divergences are treated by the introduction of a small fictitious mass δ for the photon, which we shall explain in the next section.

The typical Feynman diagrams for the virtual corrections of order α are listed in Figs. 2.1–2.16. These contributions have to be supplemented by the counterterm renormalizing the vertex $H^+ A^0 W^-$ (2.4). Note that in the THDM, the vertices $W^+ A^0 G^-$, $W^+ G^0 H^-$, $W^+ W^- A^0$ and $A^0 H^+ H^-$ are not present, and so the mixing G^+–H^+, G^0–A^0 and W^+–H^+ does not give any contribution to our process. In our case, the gauge boson W is on-shell and so the mixing $W^\pm$–$G^\mp$ is absent. The full set of Feynman diagrams are generated and computed using the FeynArts and FeynCalc [23,24] packages. The amplitudes of the typical vertices are given in terms of the one-loop scalar functions [25] and are written explicitly in Appendix B. We also use the fortran FF-package [26] in the numerical analysis.

In what follows we will use the on-shell renormalization scheme developed in [19] (and references therein). The vertex counterterm is given by

$$\delta\mathcal{L} = \frac{e}{2s_{\mathrm{W}}} W^+_\mu (H^- \overset{\leftrightarrow}{\partial}{}^\mu A^0) \qquad (2.4)$$

$$\times \left(\frac{1}{2} \delta Z_{WW} + \frac{1}{2} \delta Z_{A^0 A^0} + \frac{1}{2} \delta Z_{H^\pm H^\pm} + \delta Z_e - \frac{\delta s_{\mathrm{W}}}{s_{\mathrm{W}}} \right),$$

where δZ_{WW}, $\delta Z_{A^0 A^0}$ and $\delta Z_{H^\pm H^\pm}$ are the wave function renormalization constants for the $W^\pm$ gauge boson, A^0
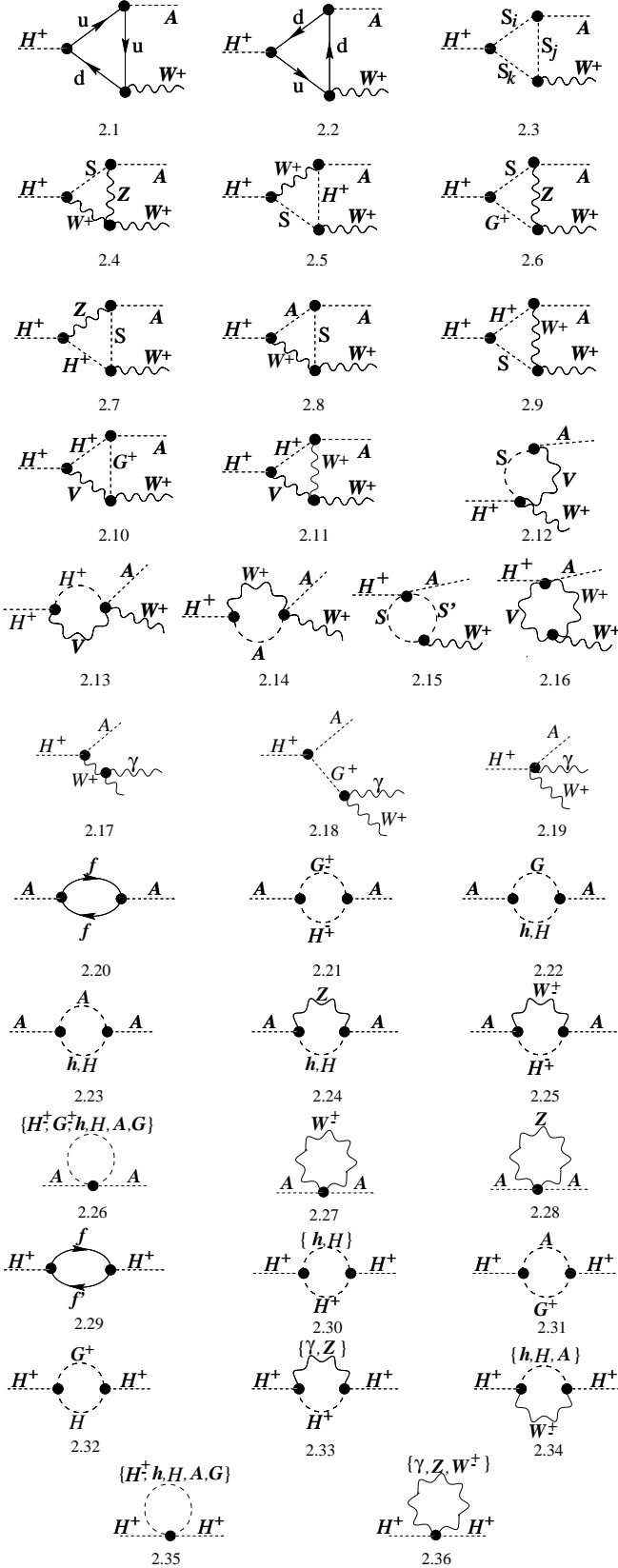
Fig. 2. Feynman diagrams for the one-loop corrections to the decay $H^+ \to A^0 W^+$: (i) vertex (2.1–2.16), (ii) bremsstrahlung diagrams for $H^+ \to A^0 W^+ \gamma$ (2.17–2.19) (iii) CP-odd Higgs boson self-energy (2.20–2.28) and charged Higgs boson self-energy (2.29–2.36)

and $H^\pm$ Higgs boson, defined as follows:

$$\delta Z_{ii} = -\left.\frac{\partial \Sigma_{ii}(k^2)}{\partial k^2}\right|_{k^2=m_i^2}, \quad i = W, A^0, H^\pm, \quad (2.5)$$

$$\delta m_i^2 = \mathrm{Re}\, \Sigma_{ii}(m_i^2), \quad i = W, Z. \quad (2.6)$$

where $\Sigma_{ii}(k^2)$ is the bare self-energy of the $H^\pm$, A^0 or W. The electric charge counterterm and $\delta s_{\mathrm{W}}/s_{\mathrm{W}}$ are defined by

$$\frac{\delta s_{\mathrm{W}}}{s_{\mathrm{W}}} = -\frac{1}{2}\frac{c_{\mathrm{W}}^2}{s_{\mathrm{W}}^2}\left(\frac{\delta m_W^2}{m_W^2} - \frac{\delta m_Z^2}{m_Z^2}\right), \quad (2.7)$$

$$\delta Z_e = -\frac{1}{2}\delta Z_{\gamma\gamma} + \frac{1}{2}\frac{s_{\mathrm{W}}}{c_{\mathrm{W}}}\delta Z_{Z\gamma}$$

$$= \frac{1}{2}\left.\frac{\partial \Sigma_{\mathrm{T}}^{\gamma\gamma}(k^2)}{\partial k^2}\right|_{k^2=0} + \frac{s_{\mathrm{W}}}{c_{\mathrm{W}}}\frac{\Sigma_{\mathrm{T}}^{\gamma Z}(0)}{m_Z^2}. \quad (2.8)$$

The index T in $\Sigma_{\mathrm{T}}^{\gamma\gamma}$ and $\Sigma_{\mathrm{T}}^{\gamma Z}$ denotes that we take the transverse part. The scalar one-loop self-energies entering in the above equations (2.5)–(2.8) are given in Appendix C.1 and C.2, while the gauge boson self-energies can be found in [27].

The one-loop amplitude $\mathcal{M}^1$ (vertex plus counterterms) can be written

$$\mathcal{M}^1(H^+ \to W^+ A^0) = \frac{e}{2s_{\mathrm{W}}}(\Gamma_H p_H^\mu + \Gamma_W p_W^\mu)\epsilon_\mu^*, \quad (2.9)$$

where Γ_H and Γ_W can be cast as follows:

$$\Gamma_W = \Gamma_W^{\mathrm{vertex}} + \delta\Gamma_W^{\mathrm{vertex}}, \quad (2.10)$$

$$\Gamma_H = \Gamma_H^{\mathrm{vertex}} + \delta\Gamma_H^{\mathrm{vertex}}. \quad (2.11)$$

Here $\Gamma_{W,H}^{\mathrm{vertex}}$ represents the vertex corrections and $\delta\Gamma_{W,H}^{\mathrm{vertex}}$ is the counterterm contribution needed to remove the UV divergences contained in $\Gamma_{W,H}^{\mathrm{vertex}}$.

The expressions of the counterterms are

$$\delta\Gamma_W^{\mathrm{vertex}} = -\left(\delta Z_e - \frac{\delta s_{\mathrm{W}}}{s_{\mathrm{W}}}\right.$$

$$\left. + \frac{1}{2}(\delta Z_{H^+H^+} + \delta Z_{A^0} + \delta Z_W)\right),$$

$$\delta\Gamma_H^{\mathrm{vertex}} = -2\delta\Gamma_W^{\mathrm{vertex}}. \quad (2.12)$$

In the on-shell case the interference term $2\mathrm{Re}\mathcal{M}^{0*}\mathcal{M}^1$, found from squaring the one-loop corrected amplitude $|\mathcal{M}^0 + \mathcal{M}^1|^2$, is equal to $\Gamma_H|\mathcal{M}^0|^2$ [19]. Hence the one-loop corrected width Γ_{on}^1 can be written as

$$\Gamma_{\mathrm{on}}^1 = (1 + \Gamma_H)\Gamma_{\mathrm{on}}^0, \quad (2.13)$$

with Γ_H defined by (2.11) interpreted as the fractional contribution to the tree-level width, Γ_{on}^0. Note that Γ_W (2.10) does not contribute to Γ_{on}^1.

3. Real photon emission: $H^+ \to W^+ A^0 \gamma$

The vertex correction supplemented by the counterterms is UV finite but there still remains infra-red divergences.

These arise from the Diagrams 2.10 and 2.11 with $V = \gamma$ and also from the wave function renormalization constant $\delta Z_{H^\pm H^\pm}$ (Diagram 2.33) and δZ_{WW}. In order to obtain a finite result, one has to add the correction from the emission of a real photon in the final state as drawn in Figs. 2.17–2.19.

In terms of the momenta of the particles in the final state, the square amplitude of the process $H^+ \to A^0 W^+ \gamma$ is given by

$$|M(H^+ \to A^0 W^+ \gamma)|^2 = -\frac{e^4}{s_{\rm W}^2} \lambda(m_{H\pm}^2, m_A^2, m_W^2)$$
$$\times \left[\frac{m_{H\pm}^2}{m_W^2} \frac{1}{(2p_H k_\gamma)^2} + \frac{1}{(2p_W k_\gamma)^2} \right.$$
$$\left. + \left(\frac{m_A^2 - m_{H\pm}^2}{m_W^2} - 1 \right) \frac{1}{(2p_W k_\gamma)(2p_H k_\gamma)} \right], \quad (3.1)$$

where k_γ denotes the momentum of the photon. Note that as a consequence of gauge invariance, the amplitude of the sum of the three diagrams (Figs. 2.17–2.19), should vanish when multiplied by the four-momentum of the photon, which provides a good check of the calculation. The integrals over three-body phase space can be found in [28], and one obtains the following expression for the width:

$$\Gamma_{\rm Br} = -\Gamma_{\rm on}^0 \frac{e^2 M_{H\pm}^2}{\pi^2 \lambda^{1/2}} \quad (3.2)$$
$$\times \left[\frac{m_{H\pm}^2}{m_W^2} I_{HH} + I_{WW} + \left(1 + \frac{m_{H\pm}^2 - m_A^2}{m_W^2} \right) I_{HW} \right],$$

where I_{HH}, I_{WW} and I_{HW} are given by

$$I_{HH} = \frac{1}{4m_{H\pm}^4} \left\{ \lambda^{1/2} \log\left(\frac{\lambda}{\delta m_{H\pm} m_A m_W} \right) \right.$$
$$\left. - \lambda^{1/2} - (m_W^2 - m_A^2) \log\left(\frac{\beta_1}{\beta_2} \right) - m_{H\pm}^2 \log(\beta_0) \right\},$$

$$I_{WW} = \frac{1}{4m_{H\pm}^2 m_W^2} \left\{ \lambda^{1/2} \log\left(\frac{\lambda}{\delta m_{H\pm} m_A m_W} \right) \right.$$
$$\left. - \lambda^{1/2} - (m_{H\pm}^2 - m_A^2) \log\left(\frac{\beta_0}{\beta_2} \right) - m_W^2 \log(\beta_1) \right\},$$

$$I_{HW} = \frac{1}{4m_{H\pm}^4} \left\{ 2\log\left(\frac{\lambda}{\delta m_{H\pm} m_A m_W} \right) \log(\beta_2) \right.$$
$$+ 2\log^2(\beta_2) - \log^2(\beta_0) - \log^2(\beta_1)$$
$$\left. + 2{\rm Sp}(1 - \beta_2^2) - {\rm Sp}(1 - \beta_0^2) - {\rm Sp}(1 - \beta_1^2) \right\}, \quad (3.3)$$

where $\lambda = \lambda(m_{H\pm}^2, m_A^2, m_W^2)$ is the two-body phase space, δ is a small fictitious photon mass, Sp is the dilogarithm function and the β_i are defined by

$$\beta_0 = \frac{m_{H\pm}^2 - m_W^2 - m_A^2 + \lambda^{1/2}}{2m_W m_A},$$
$$\beta_1 = \frac{m_{H\pm}^2 - m_W^2 + m_A^2 - \lambda^{1/2}}{2m_{H\pm} m_A},$$
$$\beta_2 = \frac{m_{H\pm}^2 + m_W^2 - m_A^2 - \lambda^{1/2}}{2m_{H\pm} m_W}. \quad (3.4)$$

We stress here that the IR divergence contained in I_{HH} (I_{WW}) is canceled by the wave function renormalization constant of the charged Higgs $H^\pm$ ($W^\pm$), while the IR divergence contained in I_{HW} is cancelled by the vertex Diagrams 2.10 and 2.11 (with $V = \gamma$). One can easily confirm that adding the virtual corrections with the bremsstrahlung diagrams yields an IR finite result. This feature has been checked both algebraically and numerically.

4. THDM scalar potential: theoretical and experimental constraints

In this section we define the THDM scalar potential that we will be using. In Appendix A we list the trilinear and quartic scalar self-couplings which are relevant to our study. Other relevant couplings involving Higgs boson interactions with gauge bosons and fermions can be found in [1]. For a full list of scalar trilinear and quartic couplings, see [29]. It has been shown [1] that the most general THDM scalar potential which is both $SU(2)_{\rm L} \otimes U(1)_Y$ and CP-invariant is given by

$$V(\Phi_1, \Phi_2) = \lambda_1(|\Phi_1|^2 - v_1^2)^2 + \lambda_2(|\Phi_2|^2 - v_2^2)^2$$
$$+ \lambda_3((|\Phi_1|^2 - v_1^2) + (|\Phi_2|^2 - v_2^2))^2$$
$$+ \lambda_4(|\Phi_1|^2 |\Phi_2|^2 - |\Phi_1^+ \Phi_2|^2)$$
$$+ \lambda_5(\text{Re}(\Phi_1^+ \Phi_2) - v_1 v_2)^2$$
$$+ \lambda_6[\text{Im}(\Phi_1^+ \Phi_2)]^2, \quad (4.1)$$

where Φ_1 and Φ_2 have weak hypercharge $Y = 1$, v_1 and v_2 are respectively the vacuum expectation values of Φ_1 and Φ_2 and the λ_i are real-valued parameters. Note that this potential violates the discrete symmetry $\Phi_i \to -\Phi_i$ softly by the dimension-two term $\lambda_5 \text{Re}(\Phi_1^+ \Phi_2)$ and has the same general structure as the scalar potential of the MSSM. One can easily prove that for $\lambda_5 = 0$ the exact symmetry $\Phi_i \to -\Phi_i$ is recovered. We note that [30] lists the complete Higgs trilinear and quartic interactions for two 6 parameter potentials, referred to as "Potential A" and "Potential B". Potential A is equivalent to our potential if $\lambda_5 \to 0$, and in this limit the Feynman rules in Appendix A are in agreement with those in [30].

After electroweak symmetry breaking, the W and Z gauge bosons acquire masses given by $m_W^2 = (1/2)g^2 v^2$ and $m_Z^2 = (1/2)(g^2 + g'^2)v^2$, where g and g' are the $SU(2)_{\rm L}$ and $U(1)_Y$ gauge couplings and $v^2 = v_1^2 + v_2^2$. The combination $v_1^2 + v_2^2$ is thus fixed by the electroweak scale through $v_1^2 + v_2^2 = (2(2^{1/2})G_{\rm F})^{-1}$, and we are left with seven free parameters in (4.1), namely the $(\lambda_i)_{i=1,\dots,6}$ and $\tan\beta = v_2/v_1$. Meanwhile, three of the eight degrees of freedom of the two Higgs doublets correspond to the three Goldstone bosons $(G^\pm, G^0)$ and the remaining five become physical Higgs bosons: H^0, h^0 (CP-even), A^0 (CP-odd) and $H^\pm$. Their masses are obtained as usual by the shift $\Phi_i \to \Phi_i + v_i$ and read [1]

$$m_A^2 = \lambda_6 v^2, \quad m_{H\pm}^2 = \lambda_4 v^2,$$
$$m_{H,h}^2 = \frac{1}{2}[A + C \pm \sqrt{(A - C)^2 + 4B^2}],$$

where

$$A = 4v_1^2(\lambda_1 + \lambda_3) + v_2^2\lambda_5, \quad B = v_1v_2(4\lambda_3 + \lambda_5)$$
$$\text{and} \quad C = 4v_2^2(\lambda_2 + \lambda_3) + v_1^2\lambda_5. \tag{4.2}$$

The angle β diagonalizes both the CP-odd and charged scalar mass matrices, leading to the physical states $H^\pm$ and A^0. The CP-even mass matrix is diagonalized by the angle α, leading to the physical states H^0, h^0, with α given by

$$\sin 2\alpha = \frac{2B}{\sqrt{(A-C)^2 + 4B^2}},$$
$$\cos 2\alpha = \frac{A-C}{\sqrt{(A-C)^2 + 4B^2}}. \tag{4.3}$$

It is then straightforward algebra to invert the previous equations to obtain the λ_i in terms of physical scalar masses, $\tan\beta$, α and λ_5:

$$\lambda_4 = \frac{g^2}{2m_W^2}m_{H^\pm}^2, \quad \lambda_6 = \frac{g^2}{2m_W^2}m_A^2,$$

$$\lambda_3 = \frac{g^2}{8m_W^2}\frac{s_\alpha c_\alpha}{s_\beta c_\beta}(m_H^2 - m_h^2) - \frac{\lambda_5}{4}, \tag{4.4}$$

$$\lambda_1 = \frac{g^2}{8c_\beta^2 m_W^2}\left[c_\alpha^2 m_H^2 + s_\alpha^2 m_h^2 - \frac{s_\alpha c_\alpha}{\tan\beta}(m_H^2 - m_h^2)\right]$$
$$- \frac{\lambda_5}{4}(-1 + \tan^2\beta), \tag{4.5}$$

$$\lambda_2 = \frac{g^2}{8s_\beta^2 m_W^2}[s_\alpha^2 m_H^2 + c_\alpha^2 m_h^2 - s_\alpha c_\alpha \tan\beta(m_H^2 - m_h^2)]$$
$$- \frac{\lambda_5}{4}\left(-1 + \frac{1}{\tan^2\beta}\right). \tag{4.6}$$

We are free to take as seven independent parameters $(\lambda_i)_{i=1,\dots,6}$ and $\tan\beta$ or equivalently the four scalar masses, $\tan\beta$, α and one of the λ_i. In what follows we will take λ_5 as a free parameter. In our analysis we also take into account the following constraints when the independent parameters are varied:

(1) The contributions to the $\delta\rho$ parameter from the Higgs scalars [31] should not exceed the current limits from precision measurements [32]: $-0.0017 \le \delta\rho \le 0.0027$.

(2) From the requirement of perturbativity for the top and bottom Yukawa couplings [33], $\tan\beta$ is constrained to lie in the range $0.3 \le \tan\beta \le 130$. Upper and lower bounds have also been obtained from the experimental limits on the processes $e^+e^- \to Z^* \to h^0\gamma$ and/or $e^+e^- \to A^0\gamma$. For very light h or A^0 ($\approx 10\,\text{GeV}$) in [34] one derived $0.15 \le \tan\beta \le 75$, with the limits weakening for heavier $m_h(m_A)$. For our study we will restrict the discussion to the values $\tan\beta \ge 0.5$.

(3) We require that tree-level unitarity is not violated in a variety of Higgs scattering processes [35].

5. Numerical results and discussion

In this section we present our numerical results for Γ_H, which is the fractional correction to the tree-level width (2.13). We take the following experimental input for the physical parameters [36]. The fine structure constant: $\alpha = e^2/(4\pi) = 1/137.03598$; the gauge boson masses: $m_Z = 91.187\,\text{GeV}$, $m_W = 80.41\,\text{GeV}$; and the lepton masses: $m_e = 0.511\,\text{MeV}$, $m_\mu = 0.1057\,\text{GeV}$, $m_\tau = 1.784\,\text{GeV}$. For the light quark masses we use the effective values which are chosen in such a way that the experimentally extracted hadronic part of the vacuum polarizations is reproduced [37]:

$$m_d = 47\,\text{MeV}, \quad m_u = 47\,\text{MeV}, \quad m_s = 150\,\text{MeV},$$
$$m_c = 1.55\,\text{GeV}, \quad m_b = 4.5\,\text{GeV}.$$

For the top quark mass we take $m_t = 175\,\text{GeV}$. In the on-shell scheme we consider, $\sin^2\theta_W$ is given by $\sin^2\theta_W \equiv 1 - (m_W^2/m_Z^2)$, and this expression is valid beyond tree level.

Let us make some comment about the Yukawa corrections discussed in [19]. In the case of an on-shell W, we showed that for small $\tan\beta$ in both Model I and II one can find large corrections of up to around $\pm 10\%$ (away from threshold effects at $m_A \approx 2m_t$). In Model I for large $\tan\beta$ all fermion corrections decouple and reach a constant value of 3.3% for $\tan\beta > 4$. In Model II Γ_H is enhanced for large $\tan\beta$ (> 20) since in this scenario the internal b quarks in the loop couple more strongly to A^0. Typically for $m_{H^\pm} = 440$ one can reach a correction of about $-7\% \to -20\%$ for large $\tan\beta > 90$ and light m_A ($60 \le m_A \le 100\,\text{GeV}$). For $m_A > 100\,\text{GeV}$ the $\tan\beta$ dependence of the Yukawa correction is rather weak and lies in the range of $-5\% \to 5\%$ for $100 \le m_A \le 330\,\text{GeV}$.

We stress at this stage that in the low $\tan\beta$ ($\tan\beta < 2$) regime the corrections in Model I and Model II are practically identical. Perturbative constraints on the λ_i and unitarity constraints on the quartic scalar couplings constrain the magnitude of $\tan\beta$. As shown in [35], $\tan\beta \ge 20$ violates the unitarity bounds if $\lambda_5 = 0$, although for $\lambda_5 \ne 0$ values of $\tan\beta \ge 40$ are comfortably allowed. However, perturbative constraints on the λ_i (in particular λ_1) disfavor $\tan\beta \ge 30$ [35], and so in our analysis we will only consider small to moderate values of $\tan\beta$. Therefore our results are applicable to both Model I and II. Note that in order to satisfy the experimental constraint on $\delta\rho$ we have assumed (for the graphs we have plotted) that $\alpha = \beta - (\pi/2)$ and the charged Higgs boson mass $m_{H^\pm}$ is quasi-degenerate with m_H.

In Fig. 3 we plot Γ_H as a function of $m_{H^\pm}$ for $m_H = m_{H^\pm} - 10\,\text{GeV}$, $m_h = 120\,\text{GeV}$, $m_A = 150\,\text{GeV}$ and $\alpha = \beta - (\pi/2)$ for several values of λ_5. With the above set of parameters and for $\tan\beta = 0.5(1.5)$ and $\lambda_5 = 0$ in Fig. 3a (Fig. 3b), the unitarity constraints in the spirit of [35] require $m_{H^\pm} \le 370$ (480) GeV, with this bound weakening for increasing λ_5. This can be seen both in Fig. 3a and Fig. 3b, where we cut the curves at the value of the charged Higgs mass which violates the unitarity constraint. Both for Fig. 3a and Fig. 3b the Yukawa correction is positive
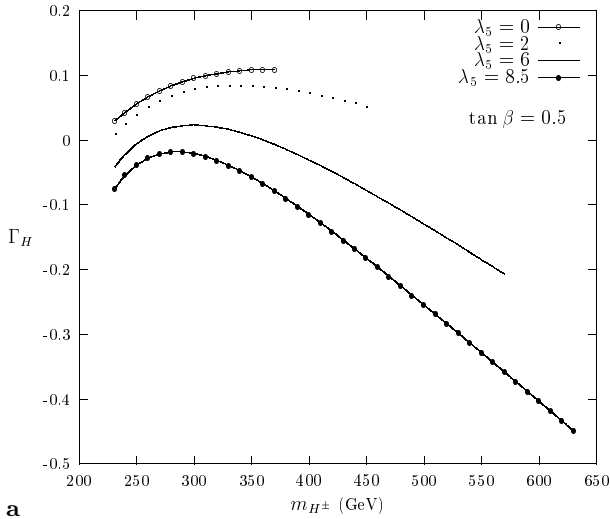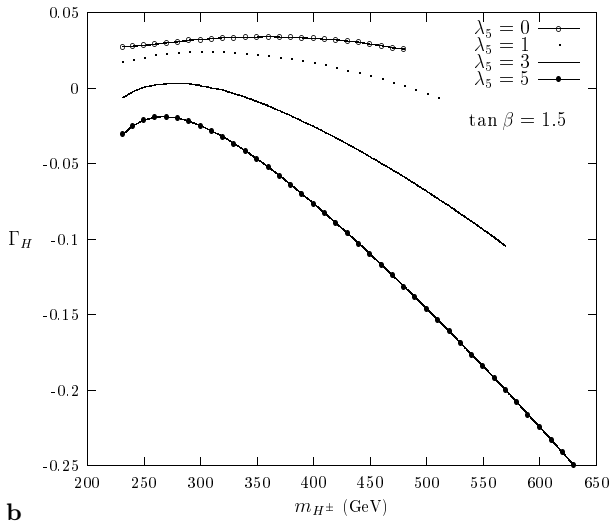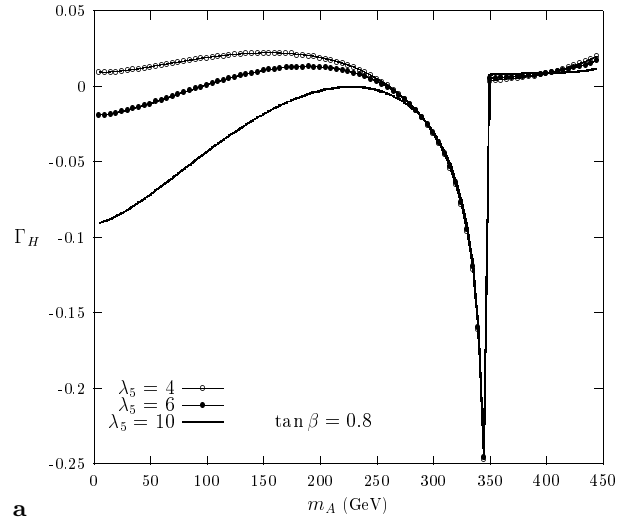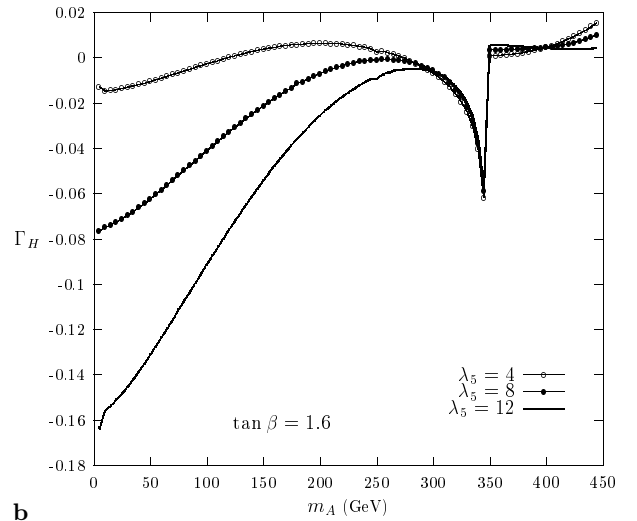
Fig. 3a,b. Total contribution to Γ_H as a function of $m_{H^\pm}$. We chose $m_H = m_{H^\pm} - 10$, $m_h = 120$, $m_A = 150$ (GeV), $\alpha = \beta - (\pi/2)$. **a** $\tan\beta = 0.5$, for the four values of λ_5=0.0, 2.0, 6.0 and 8.5. **b** $\tan\beta = 1.5$, for the four values of $\lambda_5 = 0.0$, 1.0, 3.0 and 5.0

Fig. 4a,b. Total contribution to Γ_H as a function of m_A. We chose $m_H = 500$, $m_h = 360$, $m_{H^\pm} = 530$ (GeV) and $\alpha = \beta - (\pi/2)$. **a** $\tan\beta = 0.8$, for the three values of $\lambda_5 = 4.0$, 6.0 and 10.0. **b** $\tan\beta = 1.6$, for the three values of $\lambda_5 = 4.0$, 8.0 and 12

and lies in the range $3.6\% \to 11.9\%$ and 3.3%–4.3% for Fig. 3a and Fig. 3b, respectively, while the bosonic correction is negative. In Fig. 3a ($\tan\beta = 0.5$), the bosonic correction is in the range $-0.6\% \to -0.9\%$ for $\lambda_5 = 0$ and $m_{H^\pm} \in [231, 370]$, and so in this case the Yukawa correction is dominant; for larger $\lambda_5 = 8.5$ the bosonic correction becomes strongly negative ($-11\% \to -50\%$ for $m_{H^\pm} \in [230, 620]$) and dominates the Yukawa corrections.

In Fig. 3b we take $\tan\beta = 1.5$, and the bosonic correction is in the range $-0.6\% \to -1.6\%$ for $\lambda_5 = 0$ and $m_{H^\pm} \in [230, 475]$; for $\lambda_5 = 1$ and $m_{H^\pm} \in [230, 520]$ it is in the range $-1.7\% \to -4.7\%$. In the above two cases the bosonic and Yukawa corrections interfere destructively leading to a small total correction of about $\approx 3\%$. In the case where $\lambda_5 \geq 3$ the bosonic correction becomes strongly negative and dominates the Yukawa correction.

Figures 4a,b show the total contribution to Γ_H as a function of m_A for $m_H = 500$, $m_h = 360$ and $m_{H^\pm} = 530\,\text{GeV}$. Figure 4a corresponds to $\tan\beta = 0.8$ and Fig. 4b corresponds to $\tan\beta = 1.6$ (with $\alpha = \beta - (\pi/2)$). In both figures the Yukawa correction is positive in the region $m_A \leq 277\,\text{GeV}$ and $m_A \geq 352\,\text{GeV}$, while for $m_A \approx 350\,\text{GeV}$ the channel $A \to tt$ opens, leading to a very large negative correction. Note that the bosonic correction is negative for every value of m_A.

We can conclude that for the intermediate mass range of m_A (away from threshold effects $m_A \approx 2m_t$) and for $\lambda_5 \leq 4$, there is a cancellation between the Yukawa correction and the bosonic correction. For large λ_5 the contribution to Γ_H is dominated by the bosonic correction and is consequently negative. For $m_A \approx 350\,\text{GeV}$ ($\approx 2m_t$)
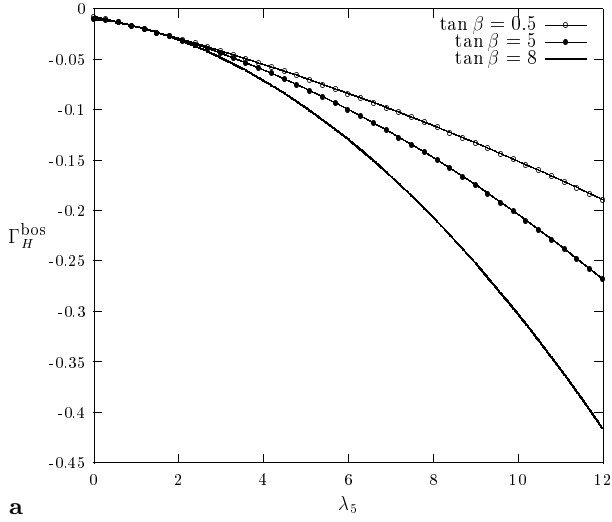
a
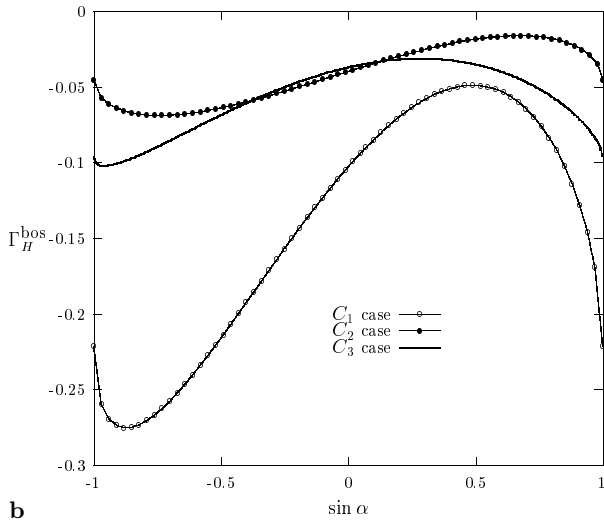
b

Fig. 5. a Bosonic contribution (Γ_H^{bos}) to Γ_H as function of λ_5. We chose $m_H = 180$, $m_h = 120$, $m_{H^\pm} = 200$, $m_A = 110$ (GeV), $\alpha = \beta - (\pi/2)$, and several values of $\tan \beta$. **b** Bosonic contribution (Γ_H^{bos}) to Γ_H as a function of $\sin \alpha$ for three different configurations C_i, $i = 1, 2, 3$: C_1: $m_{H^\pm} = 220$, $m_H = 180$, $m_h = 80$, $\tan \beta = 3.6$ and $\lambda_5 = 5$; C_2: $m_{H^\pm} = 250$, $m_H = 280$, $m_h = 140$, $\tan \beta = 1.6$ and $\lambda_5 = 5$; C_3: $m_{H^\pm} = 420$, $m_H = 400$, $m_h = 290$, $\tan \beta = 2.6$ and $\lambda_5 = 8$

there is constructive interference between the Yukawa and bosonic corrections.

In Fig. 5a we plot the bosonic contribution to Γ_H (denoted Γ_H^{bos}) as a function of λ_5 for $\tan \beta = 0.5, 5, 8$. The fermionic correction (independent of λ_5) takes the values -3.21%, 3.22%, 3.24%. One can see from the curves that Γ_H^{bos} increases with λ_5 and may approach -40%. This is expected from the form of the trilinear scalar couplings which increase linearly with λ_5.

Figure 5b shows the dependence of Γ_H^{bos} on $\sin \alpha$ for $-\pi/2 < \alpha < \pi/2$. Here C_1, C_2 and C_3 correspond to three distinct parameter configurations which satisfy both the unitarity and ρ parameter constraints (see the figure
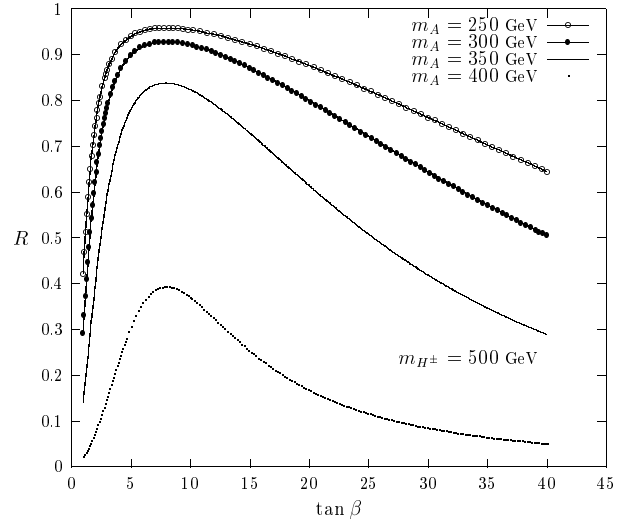

Fig. 6. Ratio R (5.1) as a function of $\tan \beta$ for various values of m_A and for $m_{H^\pm} = 500\,\text{GeV}$

caption). The fermionic corrections (independent of α) for C_1, C_2 and C_3 take the values 3.2%, 3.5% and 3.4%, respectively. The bosonic corrections become important for $\sin \alpha \approx \pm 1$.

It is apparent from the figures that Γ_H^{bos} has a complicated dependence on α, β, λ_5 and the physical Higgs masses. This is clear from the explicit form of the trilinear couplings in Appendix A.1, which mediate the numerous triangular loop corrections. Therefore enhancement in the bosonic sector may occur in a variety of scenarios. Of particular interest is the sensitivity to λ_5, a measurement of which (along with the Higgs masses and mixing angles) would allow for the reconstruction of the Higgs potential. We suggest the measurement of $\text{BR}(H^\pm \rightarrow A^0 W)$ as a way of obtaining information on λ_5. The decay mode ($H^\pm \rightarrow A^0 W$) may in fact be dominant and in Fig. 6 we show the ratio

$$R = \frac{\Gamma(H^\pm \rightarrow A^0 W)}{\Gamma(H^\pm \rightarrow A^0 W) + \Gamma(H^\pm \rightarrow tb)}$$

as a function of $\tan \beta$ for various values of m_A, fixing $m_{H^\pm} = 500\,\text{GeV}$. We plot the tree-level width for ($H^\pm \rightarrow A^0 W$) given in (2.3), and the tree-level width for $H^\pm \rightarrow tb$ given in [14], assuming Model II type couplings. Since other channels such as $H^\pm \rightarrow h^0 W$ and $H^\pm \rightarrow H^0 W$ may be open, the above ratio should be interpreted as the upper bound on $\text{BR}(H^\pm \rightarrow A^0 W)$. Note that these additional channels are suppressed by the factors $\cos^2(\beta - \alpha)$ and $\sin^2(\beta - \alpha)$, respectively, while $\Gamma(H^\pm \rightarrow A^0 W)$ possesses no mixing angle suppression. One can see that the decay $H^\pm \rightarrow A^0 W$ is maximized for moderate values of $\tan \beta$ (i.e. when $\Gamma(H^\pm \rightarrow tb)$ is minimized). The curves with lighter m_A are less phase space suppressed and so the value of R may be larger. For fixed m_A and $\tan \beta$ the sensitivity to $m_{H^\pm}$ is rather mild. A larger $m_{H^\pm}$ slightly increases R since $\Gamma(H^\pm \rightarrow A^0 W) \sim m_{H^\pm}^3$ while $\Gamma(H^\pm \rightarrow tb) \sim m_{H^\pm}$.

Given the possible large BR, an accurate measurement of BR($H^\pm \to A^0W$) may allow one to obtain information on λ_5. As explained above, the radiative corrections show sensitivity to several of the input parameters. If experimental information on the Higgs masses and mixing angles were available then it might be possible to measure λ_5. At a e^+e^- linear collider [38] one could measure the Higgs masses from a variety of production mechanisms ($e^+e^- \to Zh^0, ZH^0, h^0A^0, H^0A^0, H^+H^-$). Information on the mixing angles α, β could be obtained [39] from an analysis of the production cross sections and branching ratios. Other processes which are sensitive to λ_5 are $e^+e^- \to H^+H^-$ [5] and $H^\pm W^\mp$ [40], while theoretical bounds on the Higgs masses in the case of $\lambda_5 \neq 0$ are explored in [35,41].

6. Conclusions

We have computed the radiative corrections to the on-shell decay $H^+ \to A^0W^+$ in the general two Higgs doublet model, taking into account the experimental constraint on the ρ parameter and also unitarity constraints on the scalar sector parameters. We have included the Yukawa corrections, the full electroweak corrections (bosonic), and also the real photon emission in the final state (bremsstrahlung). The computation was done with dimensional regularization in the on-shell scheme. We find that the total radiative corrections may approach 40% in regions of parameter space for both small and moderate $\tan\beta$. The bosonic correction is sensitive to the soft discrete symmetry breaking parameter λ_5, and may interfere both constructively and destructively with the Yukawa correction. For larger λ_5 the bosonic contribution becomes strongly negative and in general dominates the Yukawa correction. For $m_A \approx 2m_t$ and low $\tan\beta$ the Yukawa correction is maximized and interferes constructively with the bosonic correction, resulting in large negative corrections to the tree-level width. Finally, we showed that the decay $H^\pm \to A^0W^\pm$ may supersede $H^\pm \to tb$ as the dominant decay channel, and thus a precise measurement of its branching ratio may allow information to be obtained on λ_5.

Appendix A:
THDM trilinear and quartic scalar couplings

In this appendix we list the Feynman rules in the general THDM for the trilinear and quartic scalar couplings relevant for our study. All formulae are written in terms of the physical masses, α, β and the soft breaking term λ_5. Note that in the trilinear couplings (quartic couplings) we have factorized out ie (ie^2). In the following $g_C = 1/(2s_W m_W s_{2\beta})$, $v^2 = 2m_W^2/g^2$, $c_{\beta\alpha}^\pm = \cos(\beta\pm\alpha)$ and $s_{\beta\alpha}^\pm = \sin(\beta\pm\alpha)$.

A.1 Trilinear scalar coupling

$$g_{H^0H^+H^-} = -2g_c(m_{H^0}^2(c_\beta^3 s_\alpha + s_\beta^3 c_\alpha)$$
$$+ m_{H^\pm}^2 s_{2\beta}c_{\beta\alpha}^- - s_{\beta\alpha}^+\lambda_5 v^2), \quad (A.1)$$

$$g_{H^0H^+G^-} = g_c s_{2\beta}s_{\beta\alpha}^-(m_{H^0}^2 - m_{H^\pm}^2), \quad (A.2)$$

$$g_{h^0H^+H^-} = -2g_c(m_{h^0}^2(c_\alpha c_\beta^3 - s_\alpha s_\beta^3) + m_{H^\pm}^2 s_{2\beta}s_{\beta\alpha}^-$$
$$- c_{\beta\alpha}^+\lambda_5 v^2), \quad (A.3)$$

$$g_{h^0H^+G^-} = -g_c s_{2\beta}c_{\beta\alpha}^-(m_{h^0}^2 - m_{H^\pm}^2), \quad (A.4)$$

$$g_{H^0A^0A^0} = -2g_c(m_{H^0}^2(s_\alpha c_\beta^3 + c_\alpha s_\beta^3)$$
$$+ m_A^2 s_{2\beta}c_{\beta\alpha}^- - s_{\beta\alpha}^+\lambda_5 v^2), \quad (A.5)$$

$$g_{H^0A^0G^0} = g_c s_{2\beta}s_{\beta\alpha}^-(m_{H^0}^2 - m_A^2), \quad (A.6)$$

$$g_{h^0A^0A^0} = -2g_c(m_{h^0}^2(c_\alpha c_\beta^3 - s_\alpha s_\beta^3) + m_A^2 s_{2\beta}s_{\beta\alpha}^-$$
$$- c_{\beta\alpha}^+\lambda_5 v^2), \quad (A.7)$$

$$g_{h^0A^0G^0} = g_c s_{2\beta}c_{\beta\alpha}^-(m_A^2 - m_{h^0}^2), \quad (A.8)$$

$$g_{A^0H^+G^-} = ig_c s_{2\beta}(m_{H^\pm}^2 - m_A^2). \quad (A.9)$$

A.2 Quartic scalar coupling

$$g_{H^0H^0H^0H^0} = -12g_C^2[m_{H^0}^2(c_\beta s_\alpha^3 + s_\beta c_\alpha^3)^2$$
$$+ m_{h^0}^2 s_\alpha^2 c_\alpha^2 s_{\beta\alpha}^{-2} - \lambda_5 v^2(c_\alpha^2 - c_\beta^2)^2], \quad (A.10)$$

$$g_{h^0h^0h^0h^0} = -12g_C^2[m_{H^0}^2 s_\alpha^2 c_\alpha^2 c_{\beta\alpha}^{-2}$$
$$+ m_{h^0}^2(c_\beta c_\alpha^3 - s_\beta s_\alpha^3)^2$$
$$- \lambda_5 v^2(c_\alpha^2 - s_\beta^2)^2], \quad (A.11)$$

$$g_{A^0A^0A^0A^0} = -12g_C^2[m_{H^0}^2(c_\alpha s_\beta^3 + s_\alpha c_\beta^3)^2$$
$$+ m_{h^0}^2(c_\alpha c_\beta^3 - s_\alpha s_\beta^3)^2 - \lambda_5 v^2 c_{2\beta}^2], \quad (A.12)$$

$$g_{G^0G^0G^0G^0} = -3g_C^2 s_{2\beta}^2[m_{H^0}^2 c_{\beta\alpha}^{-2} + m_{h^0}^2 s_{\beta\alpha}^{-2}], \quad (A.13)$$

$$g_{H^+H^-H^+H^-} = -8g_C^2[m_{H^0}^2(c_\alpha s_\beta^3 + s_\alpha c_\beta^3)^2$$
$$+ m_{h^0}^2(c_\alpha c_\beta^3 - s_\alpha s_\beta^3)^2 - \lambda_5 v^2 c_{2\beta}^2], \quad (A.14)$$

$$g_{G^+G^-G^+G^-} = -2g_C^2 s_{2\beta}^2[m_{H^0}^2 c_{\beta\alpha}^{-2} + m_{h^0}^2 s_{\beta\alpha}^{-2}], \quad (A.15)$$

$$g_{H^0H^0h^0h^0} = -4g_C^2[m_{H^0}^2 s_\alpha c_\alpha(s_\beta c_\beta + 3s_\alpha c_\alpha s_{\beta\alpha}^{-2})$$
$$- m_{h^0}^2 s_\alpha c_\alpha(s_\beta c_\beta - 3s_\alpha c_\alpha c_{\beta\alpha}^{-2})$$
$$- \lambda_5 v^2(3s_\alpha^2 c_\alpha^2 - s_\beta^2 c_\beta^2)], \quad (A.16)$$

$$g_{H^0H^0A^0A^0} = -2g_C^2[2m_{H^0}^2(s_\alpha c_\beta^3 + c_\alpha s_\beta^3)(c_\beta s_\alpha^3 + s_\beta c_\alpha^3)$$
$$+ 2m_{h^0}^2 s_\alpha c_\alpha s_{\beta\alpha}^-(c_\alpha c_\beta^3 - s_\alpha s_\beta^3)$$
$$+ m_A^2(c_\beta^2 - s_\beta^2)(c_\alpha^2 - s_\beta^2 + 2s_\alpha s_\beta c_{\beta\alpha}^-)$$
$$+ 2\lambda_5 v^2(c_{2\beta}(c_\alpha^2 s_\beta^4 - s_\alpha^2 c_\beta^4)$$
$$- s_\beta^2 c_\alpha^2(1 + s_{2\alpha}s_{2\beta}))], \quad (A.17)$$

$$g_{h^0h^0A^0A^0} = -2g_C^2[2m_{H^0}^2(s_\alpha c_\beta^3 + c_\alpha s_\beta^3)s_\alpha c_\alpha c_{\beta\alpha}^-$$
$$+ 2m_{h^0}^2(c_\beta c_\alpha^3 - s_\beta s_\alpha^3)(c_\alpha c_\beta^3 - s_\alpha s_\beta^3)$$
$$+ m_A^2(c_\beta^2 - s_\beta^2)(s_\alpha^2 + s_\beta^2 - 2s_\alpha s_\beta c_{\beta\alpha}^-)$$

$$+ 2\lambda_5 v^2(c_{2\beta}(s_\alpha^2 s_\beta^4 - c_\alpha^2 c_\beta^4)$$
$$- s_\beta^2 c_\alpha^2(1 - s_{2\alpha}s_{2\beta}))]. \tag{A.18}$$

Appendix B: One-loop vertex: $H^+ \to W A^0$

In this appendix we will list the analytic expression for each generic diagram of Fig. 2. The sum over all the particle contents yields the corresponding contribution to the one-loop amplitude for $H^+ \to W A^0$. For scalar and tensor integrals we use the same convention as [5]; the analytical expression of all scalar functions can be found in [25, 26].

B.1 Fermionic loops

The diagram with the *uud* triangle, Fig. 2.1, yields the following contribution to the one-loop amplitude:

$$M_{2.1} = -\frac{e\alpha N_C}{2\sqrt{2}\pi s_W} Y_{uu}\{Y_{ud}^L(2B_0 + B_1)$$
$$+ m_u C_0(m_u Y_{ud}^L + m_d Y_{ud}^R)$$
$$+ Y_{ud}^L[m_W^2 C_2 - 2C_{00} - 2m_A^2 C_{11}$$
$$+ C_{12}(m_{H^\pm}^2 - m_W^2 - m_A^2)]\}. \tag{B.1}$$

$N_C = 3(1)$ for quarks (leptons). Here, all the B_0, B_1, C_i and C_{ij} have the same arguments:

$$[B_0, B_1](m_{H^\pm}^2, m_u^2, m_d^2),$$
$$[C_i, C_{ij}](m_A^2, m_{H^\pm}^2, p_W^2, m_u^2, m_u^2, m_d^2).$$

The summation has to be performed over all fermion families; in practice only the third quark generation is relevant.

The corresponding expression for the the diagram with the *ddu* triangle in Fig. 2.2 is obtained from the previous one by making the replacements

$$Y_{ud}^L \longleftrightarrow Y_{ud}^R, \quad Y_{uu} \longleftrightarrow Y_{dd}, \quad m_u \longleftrightarrow m_d.$$

B.2 Bosonic loops

Diagram 2.3

$$M_{2.3} = \frac{e\alpha}{2\pi} g_{H^+ S_i S_k} g_{A S_i S_j} g_{W^+ S_j S_k}$$
$$\times C_1(m_A^2, m_{H^\pm}^2, m_W^2, m_{S_j}^2, m_{S_i}^2, m_{S_k}^2). \tag{B.2}$$

The couplings are summarized in Table 1.

Diagram 2.4

$$M_{2.4}[h] = -\frac{e\alpha c_{\bar{\beta}\alpha}^2}{16\pi s_W^3}\{-4B_0(m_{H^\pm}^2, m_h^2, m_W^2)$$

Table 1.

(S_i, S_j, S_k)	$g_{H^+ S_i S_k}$	$g_{A S_i S_j}$	$g_{W^+ S_j S_k}$
(h, A, H^+)	$g_{hH^+H^+}$	g_{hAA}	$\frac{1}{2s_W}$
(G^+, H^+, h)	$g_{hH^+G^+}$	$g_{AG^+H^+}$	$\frac{c_{\bar{\beta}\alpha}}{2s_W}$
(G^+, H^+, H)	$g_{HH^+G^+}$	$-ig_{AH^+G^+}$	$-\frac{s_{\bar{\beta}\alpha}}{2s_W}$
(G^+, H^+, A)	$-ig_{AH^+G^+}$	$-ig_{AH^+G^+}$	$\frac{1}{2s_W}$
(H, A, H^+)	$g_{HH^+H^+}$	g_{HAA}	$\frac{1}{2s_W}$
(h, G^0, G^+)	$g_{hH^+G^+}$	g_{hAG^0}	$\frac{1}{2s_W}$
(H, G^0, G^+)	$g_{HH^+G^+}$	g_{HAG^0}	$\frac{1}{2s_W}$
(A, h, G^+)	$-ig_{AH^+G^+}$	g_{hAA}	$\frac{s_{\bar{\beta}\alpha}}{2s_W}$
(A, H, G^+)	$-ig_{AH^+G^+}$	g_{HAA}	$\frac{c_{\bar{\beta}\alpha}}{2s_W}$
(H^+, G^+, h)	$g_{hH^+H^+}$	$-ig_{AH^+G^+}$	$-\frac{s_{\bar{\beta}\alpha}}{2s_W}$
(H^+, G^+, H)	$g_{HH^+H^+}$	$-ig_{AH^+G^+}$	$-\frac{c_{\bar{\beta}\alpha}}{2s_W}$

$$+ [2(-m_A^2 + m_{H^\pm}^2 - 2m_Z^2) - 4p_W^2]C_0[h]$$
$$+ [3(-m_A^2 + m_{H^\pm}^2) - 4p_W^2]C_1[h]$$
$$+ [4(-m_A^2 + m_{H^\pm}^2) - 4p_W^2]C_2[h] + 4C_{00}[h]$$
$$+ [m_{H^\pm}^2 + 3m_A^2 - p_W^2]C_{11}[h]$$
$$- 2[m_{H^\pm}^2 - m_A^2]C_{12}[h]\}, \tag{B.3}$$
$$M_{2.4}[H] = M_{2.4}[h][c_{\bar{\beta}\alpha}^2 \to s_{\bar{\beta}\alpha}^2, m_h \to m_H, h \to H], \tag{B.4}$$

where the arguments of C_i and C_{ij} are given by

$$[C_i, C_{ij}][S] = [C_i, C_{ij}](m_A^2, m_{H^\pm}^2, p_W^2, m_Z^2, m_S^2, m_W^2).$$

Diagram 2.5

$$M_{2.5}[h] = -\frac{e\alpha c_{\bar{\beta}\alpha}^2}{16\pi s_W^3}\{B_0(m_{H^\pm}^2, m_W^2, m_h^2)$$
$$+ B_1(m_{H^\pm}^2, m_W^2, m_h^2) + [p_W^2 - 2m_{H^\pm}^2]C_1[h]$$
$$+ 2C_{00}[h] + [m_{H^\pm}^2 - (p_W^2 - m_A^2)]C_{11}[h]$$
$$- [p_W^2 - m_A^2 + m_{H^\pm}^2]C_{12}[h]\}, \tag{B.5}$$
$$M_{2.5}[H] = M_{2.5}[h][c_{\bar{\beta}\alpha}^- \to s_{\bar{\beta}\alpha}^-, m_h \to m_H, h \to H], \tag{B.6}$$
$$M_{2.5}[A] = M_{2.5}[h][c_{\bar{\beta}\alpha}^2 \to -1, m_h \to m_A, h \to A], \tag{B.7}$$

where the arguments of C_i and C_{ij} are

$$[C_i, C_{ij}][S] = [C_i, C_{ij}](m_A^2, m_{H^\pm}^2, p_W^2, m_{H^\pm}^2, m_W^2, m_S^2).$$

Diagram 2.6

$$M_{2.6}[h] = \frac{e\alpha c_{\beta\alpha^-} m_W}{8\pi c_W^2} g_{h^0 H^+ G^-}(2C_0[h] + C_1[h]), \tag{B.8}$$
$$M_{2.6}[H] = M_{2.6}[h][c_{\bar{\beta}\alpha}^- \to -s_{\bar{\beta}\alpha}^-, h \to H]. \tag{B.9}$$

Here C_0 and C_1 have the same arguments:

$$[C_0, C_1][S] = [C_0, C_1](m_A^2, m_{H^\pm}^2, p_W^2, m_Z^2, m_S^2, m_W^2).$$

Diagram 2.7

$$M_{2.7}[h] = -\frac{e\alpha(c_W^2 - s_W^2)c_{\beta\alpha}^{-\ 2}}{16\pi s_W^3 c_W^2}\{B_0(m_{H^\pm}^2, m_Z^2, m_{H^\pm}^2)$$
$$+ B_1(m_{H^\pm}^2, m_Z^2, m_{H^\pm}^2)$$
$$+ [p_W^2 - m_h^2 - m_{H^\pm}^2]C_1[h] + 2C_{00}[h]$$
$$+ [-p_W^2 + m_A^2 + m_{H^\pm}^2]C_{11}[h]$$
$$- [p_W^2 - m_A^2 + m_{H^\pm}^2]C_{12}[h]\}, \tag{B.10}$$
$$M_{2.7}[H] = M_{2.7}[h][c_{\beta\alpha}^- \to s_{\beta\alpha}^-, h \to H, m_h \to m_H]. \tag{B.11}$$

The arguments of C_i and C_{ij} are given by

$$[C_i, C_{ij}][S] = [C_i, C_{ij}](m_A^2, m_{H^\pm}^2, p_W^2, m_S^2, m_Z^2, m_{H^\pm}^2).$$

Diagram 2.8

$$M_{2.8}[h] = \frac{e\alpha s_{\beta\alpha}^- m_W}{8\pi s_W^2}g_{h^0 A^0 A^0}(2C_0[h] + C_1[h]), \tag{B.12}$$
$$M_{2.8}[H] = M_{2.8}[h][s_{\beta\alpha}^- \to c_{\beta\alpha}^-, h \to H, g_{h^0 A^0 A^0}$$
$$\to g_{H^0 A^0 A^0}], \tag{B.13}$$

where C_0 and C_1 have the same arguments:

$$[C_0, C_1][S] = [C_0, C_1](m_A^2, m_{H^\pm}^2, p_W^2, m_S^2, m_A^2, m_W^2).$$

Diagram 2.9

$$M_{2.9}[h] = \frac{e\alpha s_{\beta\alpha}^- m_W}{8\pi s_W^2}g_{h^0 H^+ H^-}(2C_0[h] + C_1[h]), \tag{B.14}$$
$$M_{2.9}[H] = M_{2.9}[h][s_{\beta\alpha}^- \to c_{\beta\alpha}^-, h \to H, g_{h^0 H^+ H^-}$$
$$\to g_{H^0 H^+ H^-}], \tag{B.15}$$

where C_0 and C_1 have the same arguments:

$$[C_0, C_1][S] = [C_0, C_1](m_A^2, m_{H^\pm}^2, p_W^2, m_W^2, m_{H^\pm}^2, m_S^2).$$

Diagram 2.10

$$M_{2.10}[Z] = -\frac{e\alpha(c_W^2 - s_W^2)m_W}{8\pi c_W^2}$$
$$\times g_{A^0 H^+ G^-}(2C_0[Z] + C_1[Z]), \tag{B.16}$$
$$M_{2.10}[\gamma] = \frac{e\alpha m_W}{4\pi}g_{A^0 H^+ G^-}(2C_0[\delta] + C_1[\delta]). \tag{B.17}$$

Again the C_0 and C_1 have the same arguments:

$$[C_0, C_1][V] = [C_0, C_1](m_A^2, m_{H^\pm}^2, p_W^2, m_W^2, m_{H^\pm}^2, m_V^2).$$

Here δ is a small photon mass introduced to regularize the infrared divergence contained in the C_0 function.

Diagram 2.11

$$M_{2.11}[Z] = \frac{e\alpha(c_W^2 - s_W^2)}{16\pi s_W^3}(4B_0(m_{H^\pm}^2, m_Z^2, m_{H^\pm}^2)$$
$$+ [2p_W^2 + m_A^2 - m_{H^\pm}^2 + 2m_W^2]2C_0[Z],$$
$$+ [4p_W^2 + 3(m_A^2 - m_{H^\pm}^2)]C_1[Z]$$
$$+ [p_W^2 + m_A^2 - m_{H^\pm}^2)]4C_2[Z] - 4C_{00}[Z]$$
$$+ [p_W^2 - m_{H^\pm}^2 - 3m_A^2]C_{11}[Z]$$
$$+ [m_{H^\pm}^2 - m_A^2]2C_{12}[Z]), \tag{B.18}$$
$$M_{2.11}[\gamma] = M_{2.11}[Z]\left[\frac{(c_W^2 - s_W^2)}{s_W^2} \to 2, m_Z \to \delta\right]. \tag{B.19}$$

All C_i and C_{ij} have the same arguments:

$$[C_i,\ C_{ij}][V] = [C_i,\ C_{ij}](m_A^2, m_{H^\pm}^2, p_W^2, m_W^2, m_{H^\pm}^2, m_V^2).$$

Diagram 2.12

$$M_{2.12}[h, Z] = -\frac{e\alpha c_{\beta\alpha}^{-\ 2}}{16\pi s_W c_W^2}(2B_0(m_A^2, m_Z^2, m_h^2)$$
$$+ B_1(m_A^2, m_Z^2, m_h^2)), \tag{B.20}$$
$$M_{2.12}[H^+, W^+] = -\frac{e\alpha}{16\pi s_W^3}(2B_0(m_A^2, m_W^2, m_{H^\pm}^2)$$
$$+ B_1(m_A^2, m_W^2, m_{H^\pm}^2)), \tag{B.21}$$
$$M_{2.12}[H, Z] = -\frac{e\alpha s_{\beta\alpha}^{-\ 2}}{16\pi s_W c_W^2}(2B_0(m_A^2, m_Z^2, m_H^2)$$
$$+ B_1(m_A^2, m_Z^2, m_H^2)). \tag{B.22}$$

Diagram 2.13

$$M_{2.13}[Z] = \frac{e\alpha(c_W^2 - s_W^2)}{16\pi s_W c_W^2}(B_0(m_{H^\pm}^2, m_{H^\pm}^2, m_Z^2)$$
$$- B_1(m_{H^\pm}^2, m_{H^\pm}^2, m_Z^2)), \tag{B.23}$$
$$M_{2.13}[\gamma] = -\frac{e\alpha}{8\pi s_W}(B_0(m_{H^\pm}^2, m_{H^\pm}^2, \delta)$$
$$- B_1(m_{H^\pm}^2, m_{H^\pm}^2, \delta)). \tag{B.24}$$

Diagram 2.14

$$M_{2.14} = -\frac{e\alpha}{16\pi s_W^3}(2B_0(m_{H^\pm}^2, m_W^2, m_A^2)$$
$$+ B_1(m_{H^\pm}^2, m_W^2, m_A^2)). \tag{B.25}$$

Diagram 2.15 and 2.16

For this kind of topology, it is clear that the amplitude is proportional to the W gauge boson momentum (Lorentz invariance) and consequently for the W on-shell the amplitude vanishes:

$$M_{2.15} = 0, \quad M_{2.16} = 0. \tag{B.26}$$

Appendix C: Charged and CP-odd Higgs bosons self-energies

This appendix is devoted to the self-energies of the charged and CP-odd Higgs bosons which are needed for the on-shell renormalization scheme. The gauge bosons self-energies γ–γ, γ–Z, Z–Z and W–W can be found in [27].

C.1 CP-odd Higgs boson self-energy

The CP-odd Higgs self-energy Σ^{AA} can be cast into three parts: (i) a fermionic part, 2.20, (ii) a pure scalar part, 2.21, 2.22, 2.23 and 2.26, and (iii) a mixing of gauge boson and scalar, 2.24, 2.25, 2.27 and 2.28, in such a way that

$$\Sigma^{AA}(q^2) = \Sigma_f^{AA}(q^2) + \Sigma_S^{AA}(q^2) + \Sigma_{VS}^{AA}(q^2), \quad \text{(C.1)}$$

with

$$\Sigma_f^{AA}(q^2) = -\frac{\alpha N_C}{\pi} Y_{ff}^2 (A_0(m_f^2) + q^2 B_1(q^2, m_f^2, m_f^2)), \quad \text{(C.2)}$$

$$\begin{aligned}
\Sigma_S^{AA}(q^2) = &\frac{\alpha}{4\pi}(g_{hAA}^2 B_0(q^2, m_A^2, m_h^2) \\
&+ g_{HAA}^2 B_0(q^2, m_A^2, m_H^2) \\
&+ g_{hAG}^2 B_0(q^2, m_h^2, m_Z^2) + g_{HAG}^2 B_0(q^2, m_H^2, m_Z^2) \\
&+ 2g_{AH^+G^-}^2 B_0(q^2, m_{H^\pm}^2, m_W^2)) \\
&+ \frac{\alpha}{8\pi}\left(-g_{AAAA}A_0(m_A^2) - g_{hhAA}A_0(m_h^2) \right. \\
&- g_{HHAA}A_0(m_H^2) - 2g_{H^+H^-AA}A_0(m_{H^\pm}^2) \\
&- 2g_{G^+G^-AA}A_0(m_W^2) \\
&- g_{AAGG}A_0(m_Z^2) + \frac{2}{s_W^2 c_W^2}A_0(m_Z^2) \\
&\left. + \frac{4}{s_W^2}A_0(m_W^2) - \frac{2}{s_W^2}m_W^2 - \frac{1}{s_W^2 c_W^2}m_Z^2 \right), \quad \text{(C.3)}
\end{aligned}$$

$$\begin{aligned}
\Sigma_{VS}^{AA}(q^2) = &-\frac{\alpha}{16\pi c_W^2 s_W^2} \\
&\times (c_{\beta\alpha}^{-\,2}(A_0(m_Z^2) + (m_h^2 + q^2)B_0(q^2, m_h^2, m_Z^2) \\
&- 2q^2 B_1(q^2, m_h^2, m_Z^2)) \\
&+ s_{\beta\alpha}^{-\,2}(A_0(m_Z^2) + (m_H^2 + q^2)B_0(q^2, m_H^2, m_Z^2) \\
&- 2q^2 B_1(q^2, m_H^2, m_Z^2)) + c_W^2(A_0(m_W^2) \\
&+ (m_{H^\pm}^2 + q^2)B_0(q^2, m_{H^\pm}^2, m_W^2) \\
&- 2q^2 B_1(q^2, m_{H^\pm}^2, m_W^2))). \quad \text{(C.4)}
\end{aligned}$$

C.2 Charged Higgs boson self-energy

The charged Higgs boson self-energy $\Sigma^{H^+H^-}$ can be cast into three parts: (i) a fermionic part, 2.29, (ii) a pure scalar part 2.30, 2.31, 2.32 and 2.35, and (iii) a mixing of gauge boson and scalar, 2.33, 2.34 and 2.36, in such a way that

$$\Sigma^{H^+H^-}(q^2) = \Sigma_f^{H^\pm H^\pm}(q^2) + \Sigma_S^{H^+H^-}(q^2) + \Sigma_{VS}^{H^+H^-}(q^2), \quad \text{(C.5)}$$

$$\begin{aligned}
\Sigma_{ff'}^{H^\pm H^\pm}(q^2) = &-\frac{\alpha N_C}{2\pi}((Y_{ff'}^{L\,2} + Y_{ff'}^{R\,2}) \\
&\times (A_0(m_f^2) + q^2 B_1(q^2, m_{f'}^2, m_f^2)) \\
&+ (m_{f'}^2(Y_{ff'}^{L\,2} + Y_{ff'}^{R\,2}) \\
&+ 2m_{f'}m_f Y_{ff'}^L Y_{ff'}^R)B_0(q^2, m_{f'}^2, m_f^2)), \quad \text{(C.6)}
\end{aligned}$$

$$\begin{aligned}
\Sigma_S^{H^\pm H^\pm}(q^2) = &\frac{\alpha}{4\pi}(g_{AH^+G^-}^2 B_0(q^2, m_A^2, m_W^2) \\
&+ g_{hH^+H^-}^2 B_0(q^2, m_h^2, m_{H^\pm}^2) \\
&+ g_{hH^+G^-}^2 B_0(q^2, m_h^2, m_W^2) \\
&+ g_{HH^+H^-}^2 B_0(q^2, m_H^2, m_{H^\pm}^2) \\
&+ g_{HH^+G^-}^2 B_0(q^2, m_H^2, m_W^2)) \\
&- \frac{\alpha}{8\pi}\left(g_{H^+H^-AA}A_0(m_A^2) + g_{H^+H^-hh}A_0(m_h^2) \right. \\
&+ g_{H^+H^-HH}A_0(m_H^2) \\
&+ 2g_{H^+H^-H^+H^-}A_0(m_{H^\pm}^2) \\
&+ \frac{2}{s_W^2}(m_W^2 - 2A_0(m_W^2)) \\
&+ g_{H^+H^-GG}A_0(m_Z^2) \\
&\left. + \frac{(s_W^2 - c_W^2)^2}{c_W^2 s_W^2}(m_Z^2 - 2A_0(m_Z^2)) \right), \quad \text{(C.7)}
\end{aligned}$$

$$\begin{aligned}
\Sigma_{VS}^{H^\pm H^\pm}(q^2) = &-\frac{\alpha}{16\pi s_W^2} \\
&\times \left(4s_W^2((m_{H^\pm}^2 + q^2)B_0(q^2, 0, m_{H^\pm}^2) \right. \\
&- 2q^2 B_1(q^2, m_{H^\pm}^2, 0)) \\
&+ \frac{(c_W^2 - s_W^2)^2}{c_W^2} \\
&\times (A_0(m_Z^2) + (m_{H^\pm}^2 + q^2)B_0(q^2, m_{H^\pm}^2, m_Z^2) \\
&- 2q^2 B_1(q^2, m_{H^\pm}^2, m_Z^2)) \\
&+ (A_0(m_A^2) + (m_W^2 + 4q^2)B_0(q^2, m_A^2, m_W^2) \\
&+ 4q^2 B_1(q^2, m_W^2, m_A^2)) + c_{\beta\alpha}^{-\,2}(A_0(m_h^2) \\
&+ (m_W^2 + 4q^2)B_0(q^2, m_h^2, m_W^2) \\
&+ 4q^2 B_1(q^2, m_W^2, m_h^2)) + s_{\beta\alpha}^{-\,2}(A_0(m_H^2) \\
&+ (m_W^2 + 4q^2)B_0(q^2, m_H^2, m_W^2) \\
&\left. + 4q^2 B_1(q^2, m_W^2, m_H^2))\right). \quad \text{(C.8)}
\end{aligned}$$

References

1. J.F. Gunion, H.E. Haber, G.L. Kane, S. Dawson, The Higgs hunter's guide (Addison-Wesley, Reading 1990)
2. S. Weinberg, Phys. Rev. Lett. **19**, 1264 (1967); S. Glashow, Nucl. Phys. **20**, 579 (1961); A. Salam, in Elementary Particle Theory, edited by N. Svartholm (1968) p. 367
3. J. Preskill, S.P. Trivedi, F. Wilczek, M.B. Wise, Nucl. Phys. B **363**, 207 (1991)

4. S. Komamiya, Phys. Rev. D **38**, 2158 (1988); A. Sopczak, Z. Phys. C **65**, 449 (1995); S. Moretti, K. Odagiri, J. Phys. G **23**, 537 (1997); A. Arhrib, M. Capdequi Peyranère, G. Moultaka, Phys. Lett. B **341**, 313 (1995); M.A. Diaz, Tonnis A. ter Veldhuis, hep-ph/9501315; A. Gutierrez-Rodriguez, O.A. Sampayo, hep-ph/9911361

5. A. Arhrib, G. Moultaka, Nucl. Phys. B **558**, 3 (1999)

6. E. Eichten, I. Hinchliffe, K. Lane, C. Quigg, Rev. Mod. Phys. **56**, 579 (1984); J. Gunion, H.E. Haber, F.E. Paige, W.K. Tung, S.S.D. Willenbrock, Nucl. Phys. B **294**, 621 (1987); R.M. Barnett, H.E. Haber, D.E. Soper, Nucl. Phys. B **306**, 697 (1988); D.A. Dicus, J.L. Hewett, C. Kao, T.G. Rizzo, Phys. Rev. D **40**, 787 (1989); V. Barger, R.J.N. Philips, D.P. Roy, Phys. Lett. B **324**, 236 (1994); J.L. Diaz–Cruz, O.A. Sampayo, Phys. Rev. D **50**, 6820 (1994)

7. Jiang Yi, Ma Wen-Gan, Han Liang, Han Meng, Yu Zeng-hui, J. Phys. G **24**, 83 (1998); J. Phys. G **23**, 385 (1997), erratum ibid. G **23**, 1151 (1997); A. Krause, T. Plehn, M. Spira, P.W. Zerwas, Nucl. Phys. B **519**, 85 (1998); S. Moretti, K. Odagiri, Phys. Rev. D **55**, 5627 (1997); Li Gang Jin, Chong Sheng Li, R.J. Oakes, Shou Hua Zhu, Eur. Phys. J. C **14**, 91 (2000); A.A. Barrientos Bendezu, B.A. Kniehl, Nucl. Phys. B **568**, 305 (2000); O. Brein, W. Hollik, Eur. Phys. J. C **13**, 175 (2000)

8. K. Odagiri. Phys. Lett. B **452**, 327 (1999); K. Odagiri, hep-ph/9901432;D.P. Roy, Phys. Lett. B **459**, 607 (1999); F. Borzumati, J.L. Kneur, N. Polonsky, Phys. Rev. D **60**, 115011 (1999); D.J. Miller, S. Moretti, D.P. Roy, W.J. Stirling, Phys. Rev. D **61**, 055011 (2000); S. Moretti, D.P. Roy, Phys. Lett. B **470**, 209 (1999)

9. V. Barger et al., Phys. Rep. **286**, 1 (1997); R. Alanakyan, hep-ph/9804247; A.G. Akeroyd, A. Arhrib, C. Dove, Phys. Rev. D **61**, 071702 (2000)

10. D. Bowser-Chao et al., Phys. Lett. B **315**, 313 (1995); W.G. Ma et al, Phys. Rev. D **53**, 1304 (1996); Shou Hua Zhu, Chong Sheng Li, Choung Shou Gao, Phys. Rev. D **58**, 055007 (1998)

11. For the latest combined experimental limits see: http://lephiggs.web.cern.ch/LEPHIGGS/papers/index.html

12. M. Drees, E.A. Ma, P.N. Pandita, D.P. Roy, S.K. Vempati, Phys. Lett. B **433**, 346 (1998)

13. D0 Collaboration, B. Abbott et al., Phys. Rev. Lett. **82**, 4975 (1999); CDF Collaboration, F. Abe et al, Phys. Rev. Lett. **79**, 357 (1997)

14. A. Djouadi, J. Kalinowski, P.M. Zerwas, Z. Phys. C **70**, 435 (1996)

15. A. Djouadi, J. Kalinowski, P. Ohmann, P.M. Zerwas, Z. Phys. C **74**, 93 (1997)

16. A. Pilaftsis, Phys. Lett. B **435**, 88 (1998); Phys. Rev. D **58**, 096010 (1998); A. Pilaftsis, C.E.M. Wagner, Nucl. Phys. B **553**, 3 (1999); D.A. Demir, Phys. Rev. D **60**, 055006 (1999); S.Y. Choi, J.S. Lee, Phys. Rev. D **61**, 015003 (2000)

17. A.G. Akeroyd, Nucl. Phys. B **544**, 557 (1999)

18. F.M. Borzumati, A. Djouadi, hep-ph/9806301

19. A.G. Akeroyd, A. Arhrib, E. Naimi, Eur. Phys. J. C **12**, 451 (2000); erratum ibid. C **14**, 371 (2000)

20. OPAL Collaboration, Talk given at ICHEP2000, Osaka, July 2000; http://opal.web.cern.ch/Opal/pubs/physnote/html/pn445.html

21. M. Drees, M. Guchait, D.P. Roy, Phys. Lett. B **471**, 39 (2000)

22. G. 't Hooft, M. Veltman, Nucl. Phys. B **44**, 189 (1972); P. Breitenlohner, D. Maison, Commun. Math. Phys. **52**, 11 (1977)

23. H. Eck, J. Kublbeck, Guide to FeynArts 1.0, University of Wurzburg, 1992

24. R. Mertig, Guide to FeynCalc 1.0, University of Wurzburg, 1992

25. G. Passarino, M. Veltman, Nucl. Phys. B **160**, 151 (1979); G. 't Hooft, M. Veltman, Nucl. Phys. B **153**, 365 (1979)

26. G.J. van Oldenborgh, Comput. Phys. Commun. **66**, 1 (1991)

27. A. Dabelstein, Z. Phys. C **67**, 495 (1995); P. Chankowski, S. Pokorski, J. Rosiek, Nucl. Phys. B **423**, 437 (1994); W. Hollik, C. Schappacher, Nucl. Phys. B **545**, 98 (1999)

28. A. Denner, Fortsch. Phys. **41**, 307 (1993)

29. A. Arhrib, Thèse d'Etat, University Cadi Ayyad (Marakesh, Morocco) unpublished; A. Kraft, PhD Thesis, University of Karlsruhe (Germany) unpublished

30. L. Brucher, R. Santos, Eur. Phys. J. C **12**, 87 (2000)

31. A. Denner, R.J. Guth, W. Hollik, J.H. Kuhn, Z. Phys. C **51**, 695 (1991)

32. J. Erler, P. Langacker, talk given at the 5th International Wein Symposium (WEIN 98), Santa Fe, June 1998 (hep-ph/9809352)

33. V. Barger et al., Phys. Rev. D **41**, 3421 (1990); Y. Grossman, Nucl. Phys. B **355**, 426 (1994)

34. M. Krawczyk, hep-ph/9803484, presented at Workshop on Physics at the First Muon Collider and at the Front End of the Muon Collider, Batavia, IL, 6–9 November 1997; see also hep-ph/9812536; M. Krawczyk, J. Zochowski, P. Mattig, Eur. Phys. J. C **8**, 495 (1999)

35. A. Akeroyd, A. Arhrib, E. Naimi, Phys. Lett. B **490**, 119 (2000)

36. C. Caso et al., Eur. Phys. J. C **3**, 1 (1998)

37. S. Eidelman, F. Jegerlehner, Z. Phys. C **67**, 585 (1995); H. Burkhardt, B. Pietrzyk, Phys. Lett. B **356**, 398 (1995)

38. E. Accomando et al., Phys. Rep. **299**, 1 (1998); American Linear Collider Working Group (J. Bagger et al.), hep-ex/0007022

39. J.L. Feng, T. Moroi, Phys. Rev. D **56**, 5962 (1997); V. Barger, T. Han, J. Jiang, hep-ph/0006223

40. A. Arhrib, M. Capdequi Peyranère, W. Hollik, G. Moultaka, Nucl. Phys. B **581**, 34 (2000); S. Kanemura, Eur. Phys. J. C **17**, 473 (2000); S.H. Zhu, hep-ph/9901221

41. S. Kanemura, T. Kasai, Y. Okada, Phys. Lett. B **471**, 182 (1999)